Effect of Manufacturing Process on k-Area Properties and Service Performance

Eric J. Kaufmann

Brian Metrovich

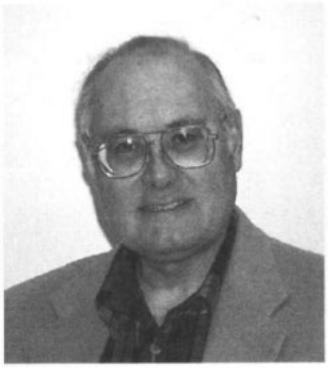

Alan W. Pense

John W. Fisher

Author

Dr. Eric J. Kaufmann is a Senior Research Engineer at the Engineering Research Center on Advanced Technology for Large Structural Systems (ATLSS) at Lehigh University where he manages the Materials and Welding Laboratories. He is a graduate of Lehigh University with B.S. and M.S. degrees in Physics and a Ph.D. degree in Materials Science and Engineering.

Author

Brian Metrovich is a research assistant at the ATLSS Engineering Research Center, Lehigh University. He received his B.S. in Civil Engineering from Ohio Northern University in 1996 and his M.S. from Lehigh University in 1999.

Author

Dr. Alan W. Pense, a member of the Lehigh University faculty since 1960, served as Chairman of the Department of Materials Science and Engineering from 1977-83, served as Dean of the College of Engineering and Applied Science, 1988-1990, and Provost and Vice President for Academic Affairs from 1990 to 1996. A graduate of Cornell University in 1957 with the Bachelor of Metallurgical Engineering degree, he received the M.S. and Ph.D. degrees from Lehigh. He is a specialist in physical and mechanical metallurgy and has conducted sponsored research on the properties and welding of materials for pressure vessels, bridges and other structures.

Author

Dr. John W. Fisher has been Professor of Civil Engineering at Lehigh University since 1969. He was Director of the Engineering Research Center on Advanced Technology for Large Structural Systems (ATLSS) since its establishment by NSF in May 1986 until September 1999 and is currently a co-director. Dr. Fisher is a graduate of Washington University, St. Louis, Missouri, with M.S.CE and Ph.D. degrees from Lehigh University. He is a member of the National Academy of Engineering and was awarded the John Fritz Medal for his researching safety and performance of steel structures for the public good.

Summary

This paper summarizes studies to characterize the properties of A36 and A572Gr50 steel section produced prior to 1984 and A572Gr50 and A913 steel sections produced in 1998. The study focused on the k-area where high levels of cold straining can occur as a result of modern rotary straightening. Charpy V-Notch (CVN) and tensile properties of the as-rolled condition and at three levels of prestrain (2%, 8% and 12%) were undertaken as well as cyclic strain tests at 2%, 4%, 6% and 8% strain range. Strain aging effects were also studied. These basic tests have demonstrated that prestraining above 2% significantly decreases the CVN absorbed energy and increases the apparent yield strength by 20-40%. The cyclic strain tests all stabilized at 2-3 cycles for the larger strain ranges. Low cycle fatigue cracking results were also acquired at 2%, 4%, and 8% strain range. In addition to the basic property tests, 20 load tests were carried out on W14x176 sections of A572Gr50 steel with 1.5 in.x12 in. HPS-70W transverse pull plates groove welded to each flange surface. Four conditions were examined including the plain rolled section, punched web holes in the k-region and continuity plates welded to the web and one flange with two gap lengths. These tests have assessed the ability of the rolled section to resist tensile forces through the k-region

EFFECT OF MANUFACTURING PROCESS ON K-AREA PROPERTIES AND SERVICE PERFORMANCE

INTRODUCTION

This paper summarizes the results of two experimental projects that have focused on the k-region of rolled column sections. The overall research program was intended to provide test data that could be used to assess the effects of manufacturing straightening procedures on the notch toughness and ductility of the k-region of rolled shapes and the ability of the sections to transmit tensile loads across the k-region. One project examined the basic mechanical properties of inelastically strained A572 Gr. 50, A913 Gr. 50 and A36 steel sections. These studies included tensile and Charpy-V-notch properties of the as-rolled sections, at three levels of pre-strain (2%, 8%, 12%), as well as cyclic inelastic strain behavior. Limited studies of the effects of strain aging were also conducted. The A36 steel section was a W36 X 260 manufactured prior to 1984 and was believed to be produced by an integrated mill. It was included in the project to compare the inelastic strain behavior of a section produced earlier by integrated mills to sections produced by current manufacturing practices. The contemporary Gr. 50 sections were W14 X 176 sections produced by three different mills. Two sections were A572 Gr. 50 and the third was A913 Gr. 50. The second project examined the strength and deformation behavior of rotarized and non-rotarized W14 X 176 column sections (A992/A572 Gr. 50) to assess their relative ability to transmit tensile loads across the k-area. The steel sections were from a single heat of steel and were either rotary straightened, gag-straightened, or left unstraightened. Tensile forces were applied to the k-area through high strength steel plates (A709 Gr. HPS-70W steel) groove welded to the column flange surface. Various fabrication conditions were also introduced which tend to localize strains within the k-area and introduce discontinuities such as holes and continuity plate weld terminations. The experimental matrix consisted of four types of specimen configurations each introducing a different strain concentration severity in the k-region for each of the three section types.

PART I - INELASTIC STRAIN BEHAVIOR OF A572 GR.50 AND A913 GR. 50 ROLLED SECTIONS

I.1 PROPERTIES OF AS-ROLLED SECTIONS

The as-rolled properties of the A572 Gr. 50, A913 Gr.50 and A36 rolled sections as well as the mill report test results are summarized in Table 1. Standard 0.505 in. round specimens located at the web mid-thickness and centerline of the section were prepared for each section. In general, the tensile properties of the A572 Gr. 50 steel (Steels A and C) were consistent with the mill certificates, however, the A913 Gr. 50 steel (Steel B) provided somewhat lower strengths which can be attributed to the mid-thickness positioning of the 0.505 in. test specimen compared to the full thickness coupon tested by the mill.

Chemical composition of the steels including residual elements are given in Table 2. The analyses show that the steels satisfy their respective specification requirements within product anlaysis tolerances. Residual element levels in Steels A, B, and C were found to be at typical levels found in modern day structural steel sections. The very low residual element levels measured in the A36 section (Steel D) provides additional evidence of its integrated mill origin.

I.2 EFFECT OF INELASTIC PRE-STRAINING

Large longitudinally oriented tensile coupons were prepared located near the web centerline of the sections for studying the effects of monotonic inelastic strain on the mechanical properties of the various steels. For each of the four rolled sections coupons were pre-strained to three different levels of strain (2%, 8%, and 12%) from which longitudinal 0.505 in. tensiles and L-T and T-L oriented Charpy V-notch specimens were then fabricated. Additional coupons were prepared from Steel A and prestrained to 8% strain for subsequent aging (10 hours) at

200 F and 400 F. Although the strain conditions introduced in the k-area during rotary straightening are a combination of tensile, compressive, and shear deformation, quantitative simulation of these complex conditions in the laboratory was not readily achievable. Consequently, monotonic tensile straining was chosen to compare the different steels and observe trends at different strain levels.

Figure 1 shows the stress-strain behavior obtained for the four steels (A, B, C, and D). The results are summarized in Figure 2 and 3 and shows that all of the steels followed the same trend. With increasing pre-strain the yield point increased by 20-40% approaching the tensile strength of the steel while tensile elongation decreased by about the same magnitude. At 12 % pre-strain, close to strain at ultimate tensile strength, yield points and tensile strengths were nearly identical as the strain hardening capacity of the steel became fully exhausted by the pre-strain.

Aging of Steel A pre-strained to 8% strain resulted in only a small additional increase in strength (~2%). Considering the low carbon (0.067%) and nitrogen (0.0032%) levels measured in this steel it is not surprising that its strain aging response was small. It is interesting that low nitrogen levels were found in all of the steels (see Table 2) and well below the A992 manufacturer's limit of 0.012%. A588 plate steels with higher nitrogen levels (0.011-0.012) studied by Herman et al (1) showed greater effect of strain aging particularly on CVN properties.

Results of Charpy V-notch (CVN) tests over the transition temperature range are shown for the as-rolled and variously pre-strained sections in Figure 4. All three contemporary sections (Steels A, B, and C) exhibited upper shelf behavior at room temperature in the as-rolled condition whereas the earlier produced A36 (Steel D) showed room temperature toughness in the transition temperature range. Pre-straining resulted in progressive reductions in absorbed energy and an upward shift in transition temperature. A summary of the shift in the 15 ft-lb transition temperature relative to the as-rolled condition ($\Delta T_{transition}$) is provided in Figure 5. For the three contemporary steel sections a pre-strain of 2% was found to shift the 15 ft-lb transition temperature 10-20 F. At 12% pre-strain the shift ranged from 40-70 F. Transverse oriented specimens consistently experienced a larger shift in transition temperature at all pre-strain levels ranging from 25-100 F. As with tensile properties the effect of aging on notch toughness was also small. An increase in transition temperature of about 15 F was observed for Steel A at the higher aging temperature compared to 68 F increase observed by Herman et al (1).

I.3 CYCLIC STRAIN BEHAVIOR

Cyclic strain tests following ASTM E606 (2) methodology were carried out on all four materials. The test specimen design utilized is shown in Figure 6. Tests were conducted at four strain range levels of 2%, 4%, 6% and 8%. Each test consisted of 10 tension-compression cycles at a single strain range. Figure 7 show a composite plot of the four individual tests performed at each strain range for the four steels. All four materials cyclically strain hardened similarly. The similarity in the cyclic strain hardening characteristics of the steels is shown in Figure 8. The stabilized cyclic stress-strain test data for each strain range is plotted and fitted to an equation of the form $\sigma = K\,\varepsilon^n$ where n is the cyclic strain hardening exponent. Also shown are the corresponding monotonic stress-strain curves for comparison. Steels A, B, and C yielded nearly the same value for n ranging from 0.096-0.111. Steel D exhibited a higher value for n of 0.150. In general, materials with greater ductility and higher cyclic strain hardening exponents show greater low cycle fatigue resistance. The test results shown in Figure 7 also show that at the lowest strain range of 2% cyclic stabilization occurred within 4-5 cycles. At the higher strain ranges all four steels cyclically stabilized within 2-3 cycles. The majority of the strain hardening appears to occur during the first strain cycle which suggests that the monotonic pre-strains used to measure effects on properties likely represents the bulk of the strain damage.

No visual indications of cracking was observed in any of the materials within the ten applied cycles. To obtain some information on crack initiation behavior several additional tests were performed where cycling was continued until initiation of fatigue cracking. Three tests were conducted at a strain range of 2%, 6% and 8% using Steel C. Cracking developed within several hundred cycles at the lowest applied strain range and within 25 cycles at 8% strain range. A strain -life plot of the results is shown in Figure 9. Extrapolating the curve to

shorter fatigue life suggests that cracking could be expected in the range of 5-10 cycles normally applied in rotary straightening at applied strain ranges of 13-18%.

PART II - TENSION LOAD TESTS ON THE K-AREA OF ROTARY STRAIGHTENED SECTIONS

II.1 ROLLED SECTION PROPERTIES

W14 X 176 sections (ASTM A992) produced from a single heat of steel were obtained from a steel manufacturer which were either rotary straightened, gag straightened or left unstraightened. The gag straightened section contained periodically spaced gag points at marked locations. Tensile properties of the three differently processed shapes were determined at the web centerline, both k-areas, and at the standard flange position as sketched in Figure 10. Coupons from the gag straightened section were centered at the gag point location marked by the manufacturer. A summary of the tensile properties is given in Table 3. Web and flange properties were found to be similar (54-56 ksi Y.S., 70-72 ksi T.S.) in all three sections. The tensile properties in the k-area of the rotary straightened section showed a sharp increase in yield strength (40%) and reduction in elongation (68%) similar to k-area properties measured in previous studies (3). The k-area stress-strain behavior for the three differently processed sections is shown in Figure 11. The rotary straightened k-area properties are consistent with 8-12% prestrained material shown in Figure 1 for prestrained web material. Interestingly, the k-area tensile properties of the gag straightened and unstraightened sections were nearly identical and similar to the web and flange tensile properties indicating that gag straightening produced no measurable change in properties in the k-area.

K-area hardness and CVN properties followed a similar trend as shown in Figure 12. Both the gag straightened and unstraightened sections showed little change in hardness through the k-region although a small increase in hardness was detected in the web-flange area in the gag straightened section. Notch toughness through the k-area was also unchanged in these sections. In contrast, the rotary straightened section provided a peak hardness in the k-area of RB 97 and a corresponding CVN energy of 5 ft-lbs at room temperature. The represents as severe a k-area condition as observed in rotary straightened sections and provides a worst case condition for the tension load tests.

II.2 TENSION LOAD TESTS

The design of the tension load test specimen is shown in Figure 13. Tensile forces were applied to the k-area of an 8 in. length of rolled section through high strength steel plates groove welded to the flange surfaces of the section. The 1.5 in. pull-plates were A709 Gr. HPS-70W with a yield strength of 87.2 ksi and tensile strength of 97.6 ksi. Four types of fabrication conditions were added in the k-area which introduced strain concentrations of varying severity in the k-region along with fabrication discontinuities. Type I configuration was the optimum configuration with no web attachments or holes. Type II configuration included a 1 in. hole located in the k-region adjacent to each flange. Types III and IV configurations had 1.5 in. stiffeners welded to the web and one flange. In one case the web groove weld terminated on the k-region (Type III) and the other case it terminated beyond the k-region as is currently recommended (4). The test matrix is summarized in Table 4. Rotary straightened sections were tested in triplicate for statistical variation resulting in a total of 20 tests. As of printing, test specimens were in preparation. Results of testing will be reported in a follow-up paper.

III. SUMMARY AND CONCLUSIONS

1. The behavior of contemporary A 572 Gr. 50 and A913 Gr.50 rolled sections under inelastic straining was found to be similar. Inelastic strains ranging from 2-12% resulted in significant changes in tensile and notch

toughness properties in all three contemporary steels studied. Yield and tensile strengths increased by 20-60% and 5-20%, respectively, with concomitant reductions in tensile elongations of 15-50%. Elevation of CVN transition temperature ranged from 20-70 F over the range of strains studied. Larger shifts in transition temperature were observed transverse to the strain direction ranging from 25-100 F.

2. Strain aging effects were found to be small in A572 Gr. 50 steel. For 8% strain a 2% increase in strength and 15 F increase in transition temperature was observed. Carbon and nitrogen levels were low in all four steels studied which may account for the small strain aging response.

3. The cyclic inelastic strain behavior of all four steels was also similar. Cyclic stabilization was achieved after 2-3 applied strain cycles for strain ranges above 2%. Low cycle fatigue cracking was not observed in any of the steels examined at strain ranges as high as 8 % in 10 applied cycles. Limited tests suggest that strain ranges of 13-18% are necessary for crack initiation to occur in 5-10 cycles normally applied in rotary straightening.

4. The k-region properties of rotary straightened sections were found to possess properties comparable to monotonic pre-strains of 8-12%.

IV. REFERENCES

1. Herman, W.A. ,Erazo, M.A., DePatto, L.R., Sekizawa, M., and Pense, A.W., "Strain Aging Behavior of Microalloyed Steels", WRC Bulletin 322, Welding Research Council, April 1987.

2. ASTM E606-92 "Standard Practice for Strain-Controlled Fatigue Testing", Vol. 03.01, ASTM, 2000.

3. "AISC Materials and Design Workshop, January 8, 1997, Chicago, IL", AISC, 1997.

4. "AISC Advisory Statement on Mechanical Properties Near the Fillet of Wide Flange Shapes and Interim Recommendations, January 10, 1997, Modern Steel Construction, AISC, February 1997.

V. ACKNOWLEDGEMENT

The authors wish to acknowledge the support of the American Institute of Steel Construction in performing this project. Also acknowledged are Nucor-Yamato Steel Co. and Bethlehem-Lukens Plate for providing test material and Leonard Kunkin Associates for fabrication of test specimens.

TABLE 1
PROPERTIES OF MATERIALS

Steel Code	Member Size	Grade	Y.S. (ksi)	T.S. (ksi)	Y/T	Elong.(2") (%)	Red. Area (%)
A	W14X176	A572 Gr. 50	58.03 [60.37]*	76.17 [78.66]	0.76	34.5 [27]	76.9
B	W14X176	A913 Gr. 50	51.08 [64.82]	70.25 [79.75]	0.73	37.8 [24]	73.0
C	W14X176	A572 Gr. 50	54.25 [55.00]	72.28 [75.00]	0.75	35.5 [23]	72.7
D	W36 X 260	A36	36.13	62.62	0.58	44.6	59.5

Notes: Standard 0.505" round specimens
Web centerline location
* Mill Test Report

TABLE 2
CHEMICAL COMPOSITIONS

Element	Composition, wt%			
	Steel A	**Steel B**	**Steel C**	**Steel D**
C	0.067	0.085	0.072	0.17
Mn	1.51	1.20	1.48	0.75
P	0.022	0.023	0.014	0.020
S	0.005	0.020	0.016	0.024
Si	0.28	0.18	0.21	0.05
Cr	0.028	0.11	0.061	0.044
Ni	0.23	0.11	0.13	0.031
Mo	0.065	0.072	0.086	0.038
Al	0.032	0.002	0.002	0.002
Cu	0.31	0.22	0.29	0.021
Co	0.001	0.010	0.008	0.004
Nb	0.003	0.008	0.003	0.002
Ti	0.002	0.001	0.001	<0.001
V	0.15	0.005	0.057	0.004
W	<0.001	<0.001	0.001	<0.001
Pb	0.006	0.003	0.011	0.003
Sn	0.004	0.013	0.013	0.002
As	0.003	0.011	0.007	0.005
Zr	0.001	0.001	0.001	<0.001
Ca	<0.001	<0.001	<0.001	<0.001
Sb	0.0034	0.0044	0.0047	<0.0001
B	<0.0001	0.0002	<0.0001	0.0001
N	0.0032	0.0033	0.0040	<0.0005
Fe	97.3	97.9	97.5	98.8

TABLE 3
TENSION LOAD TEST SECTION MECHANICAL PROPERTIES

W14 X 176	Test Location	Y.S. (ksi)	T.S. (ksi)	Elong. (8") (%)
Rotary Straightened	Web	54.14	70.34	29.7
	K-area	77.13, 82.41	85.64, 84.86	9.4, 9.4
	Flange	54.01	70.89	31.3
Gag Straightened	Web	55.06	70.39	28.9
	K-area	52.15, 53.00	69.92, 71.04	29.7
	Flange	53.92	70.99	28.9
Un-Straightened	Web	56.03	71.22	28.8
	K-area	54.18, 54.09	71.44, 70.78	29.4, 30.1
	Flange	54.92	71.87	31.3

TABLE 4
SUMMARY OF TENSION LOAD TEST CONDITIONS

Straightening Method	No. Tests			
	Specimen Configuration			
	Type I	Type II	Type III	Type IV
Rotary	3	3	3	3
Gag	1	1	1	1
None	1	1	1	1

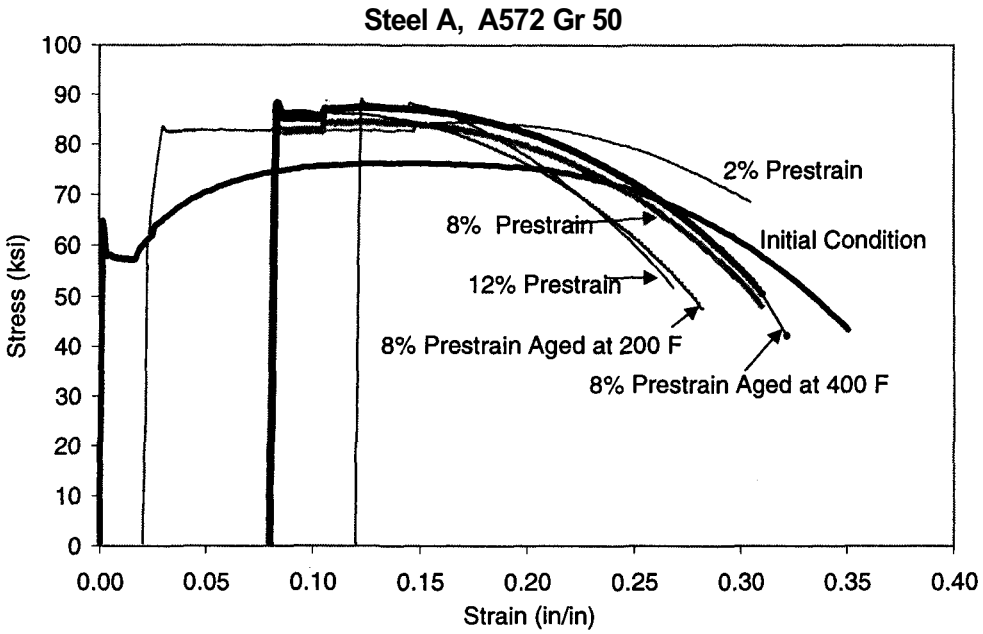

Figure 1A Stress-strain curve for Steel A under various prestrain conditions

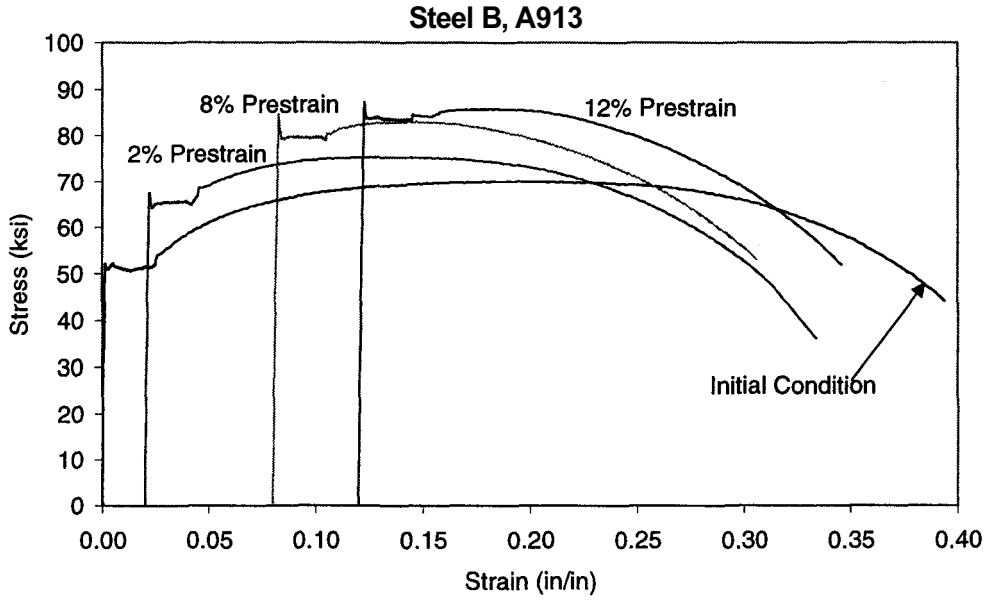

Figure 1B Stress-strain curve for Steel B under various prestrain conditions

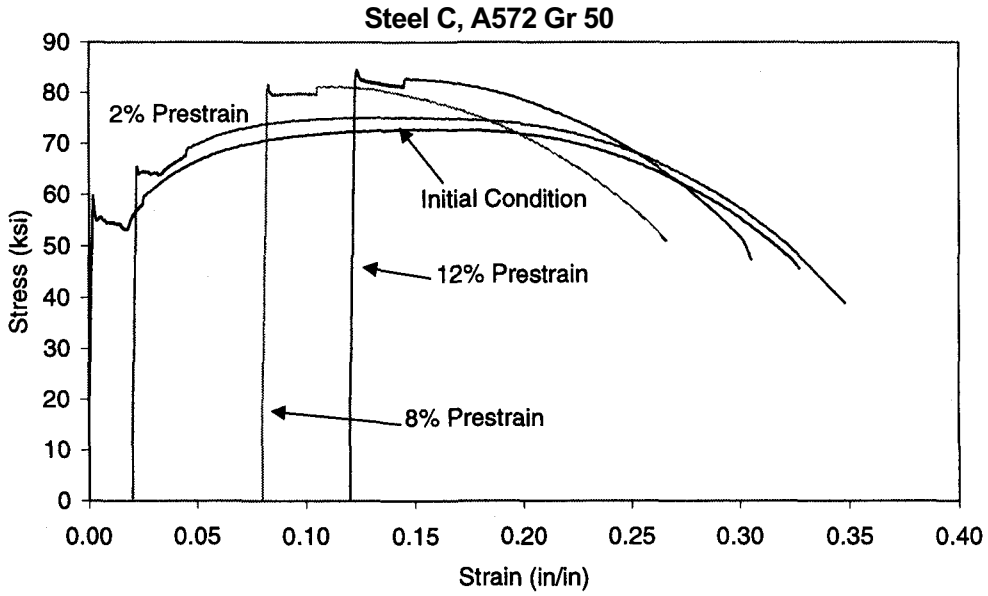

Figure 1C Stress-strain curve for Steel C under various prestrain conditions

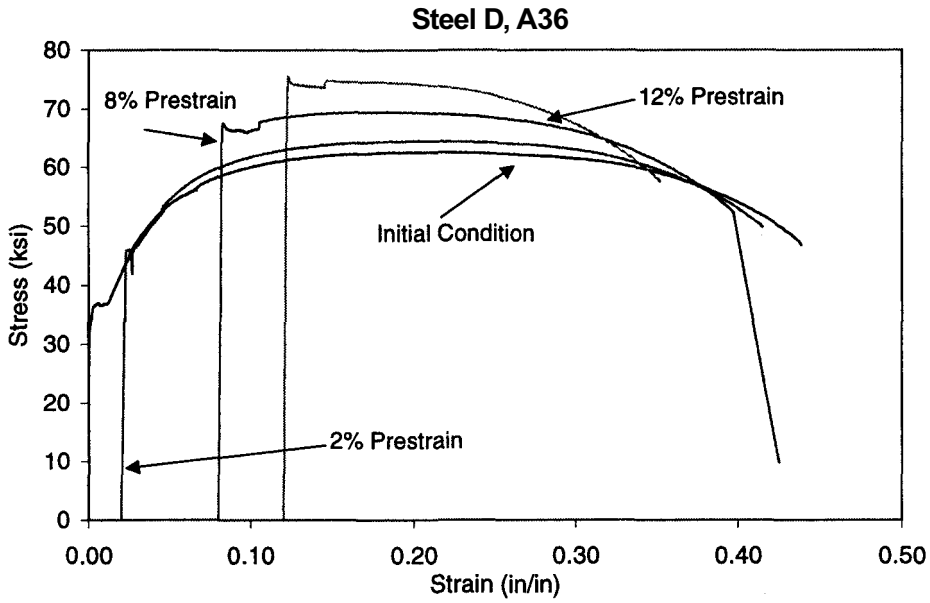

Figure 1D Stress-strain curve for Steel D under various prestrain conditions

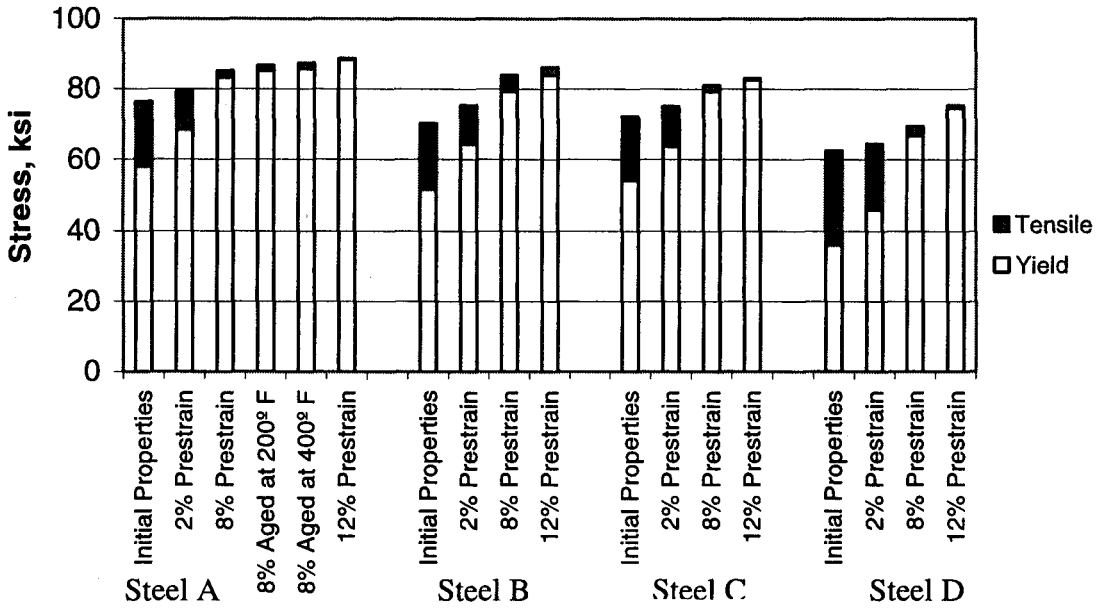

Figure 2 Yield and Tensile Strength vs. Strain Condition

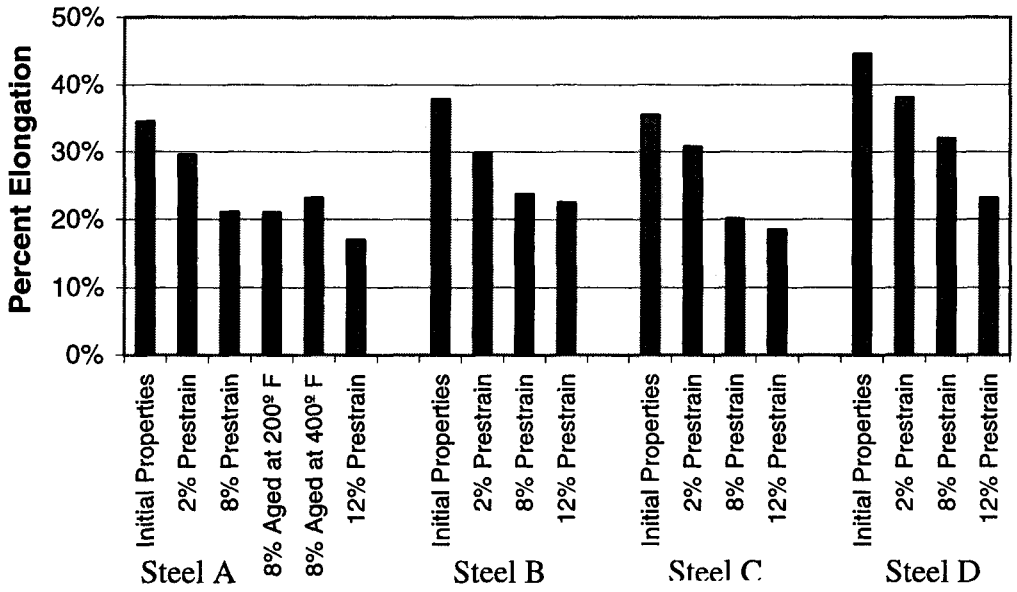

Figure 3 Percent Elongation vs. Strain Condition

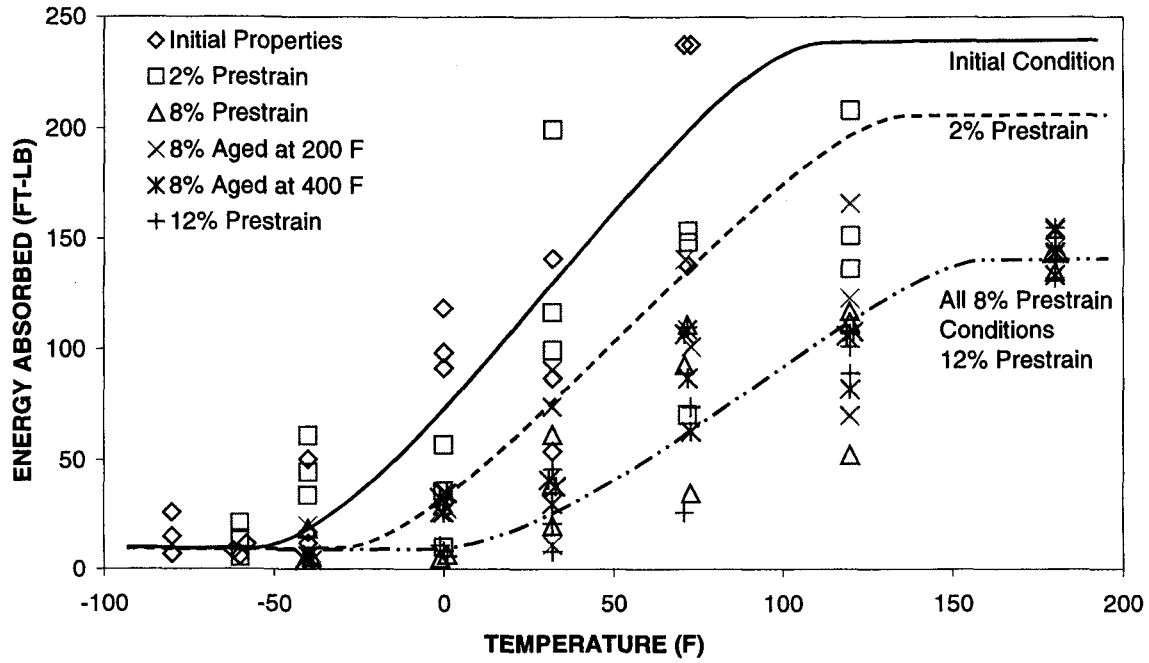

Figure 4A CVN transition curves of Steel A in the TL direction for various prestrain conditions

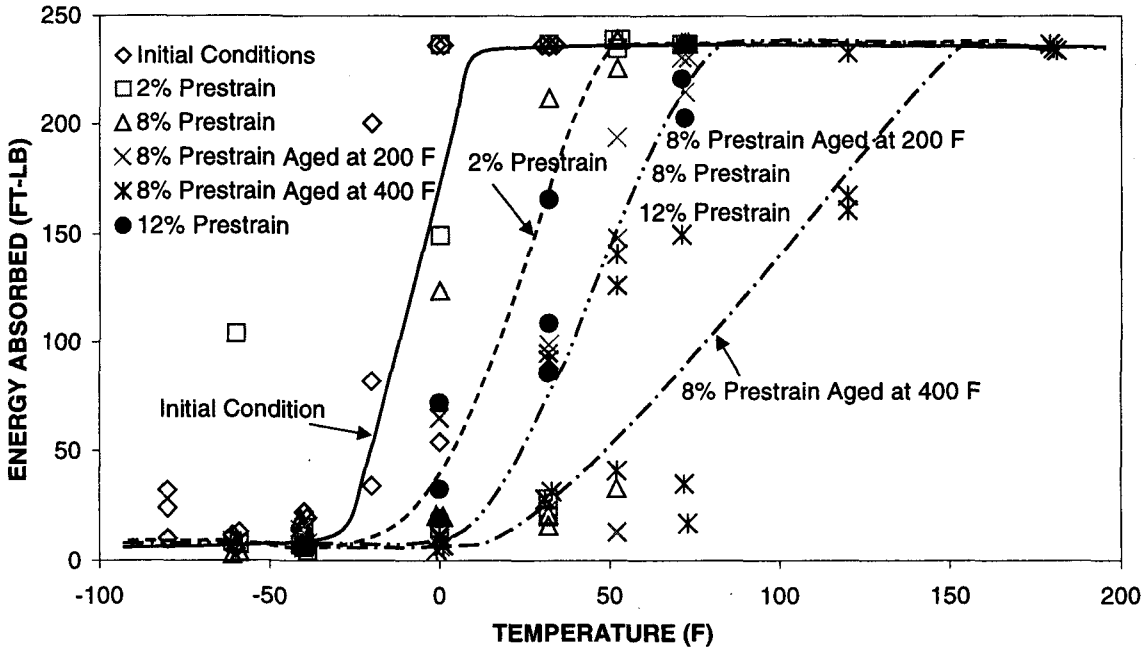

Figure 4B CVN transition curves of Steel A in the LT direction for various prestrain conditions

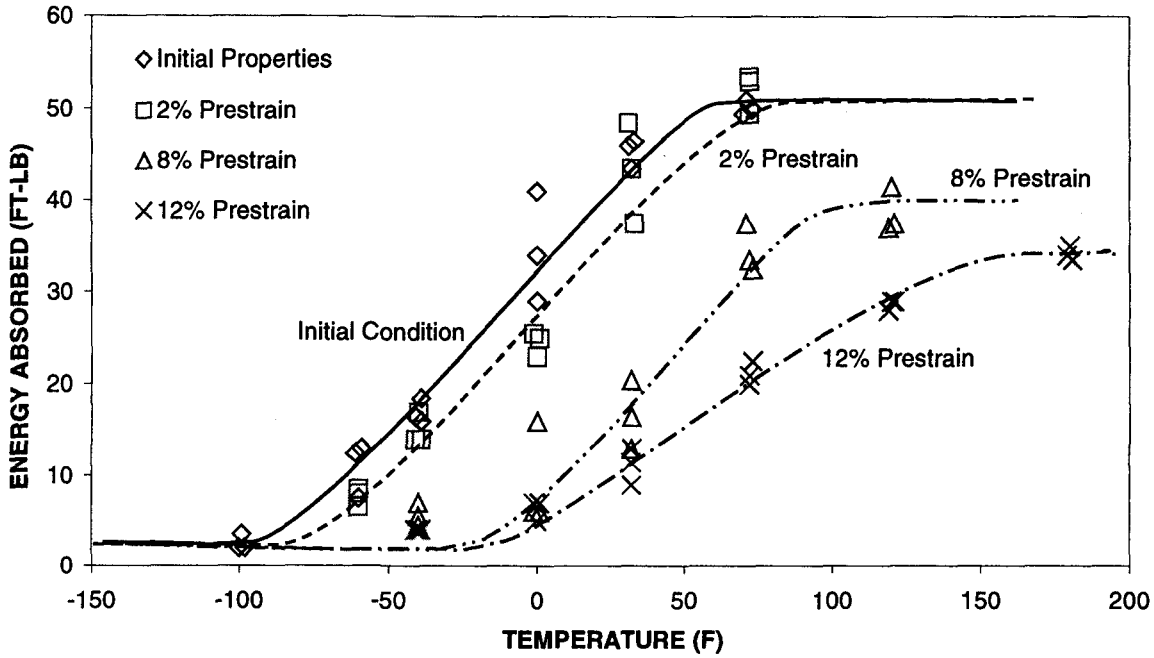

Figure 4C CVN transition curves of Steel B in the TL direction for various prestrain conditions

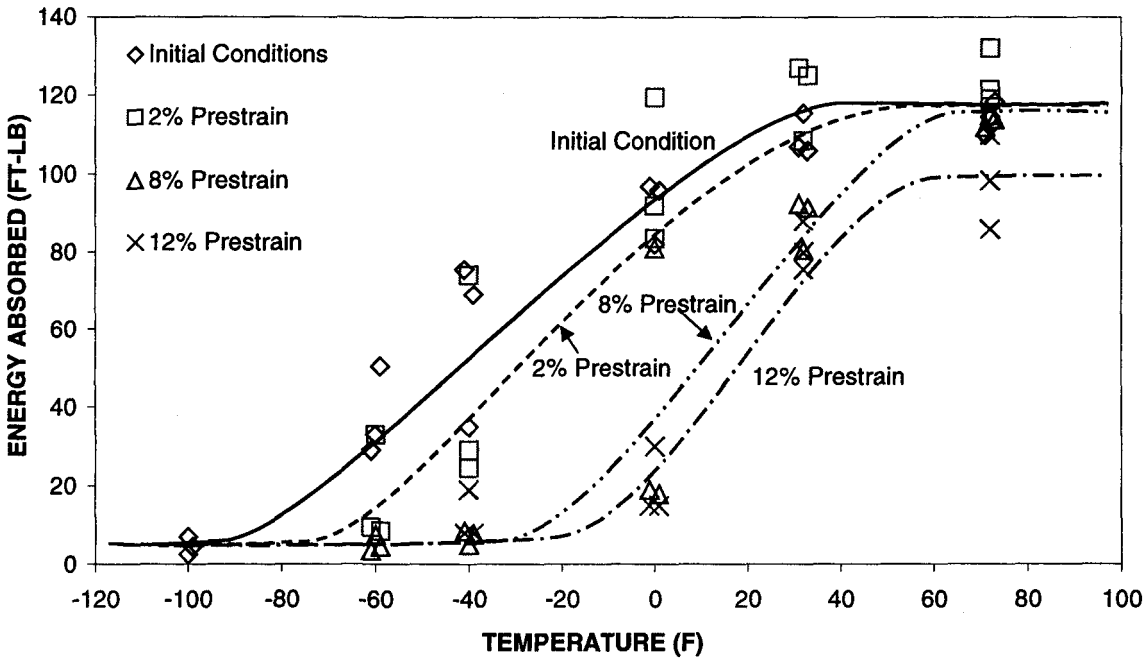

Figure 4D CVN transition curves of Steel B in the LT direction for various prestrain conditions

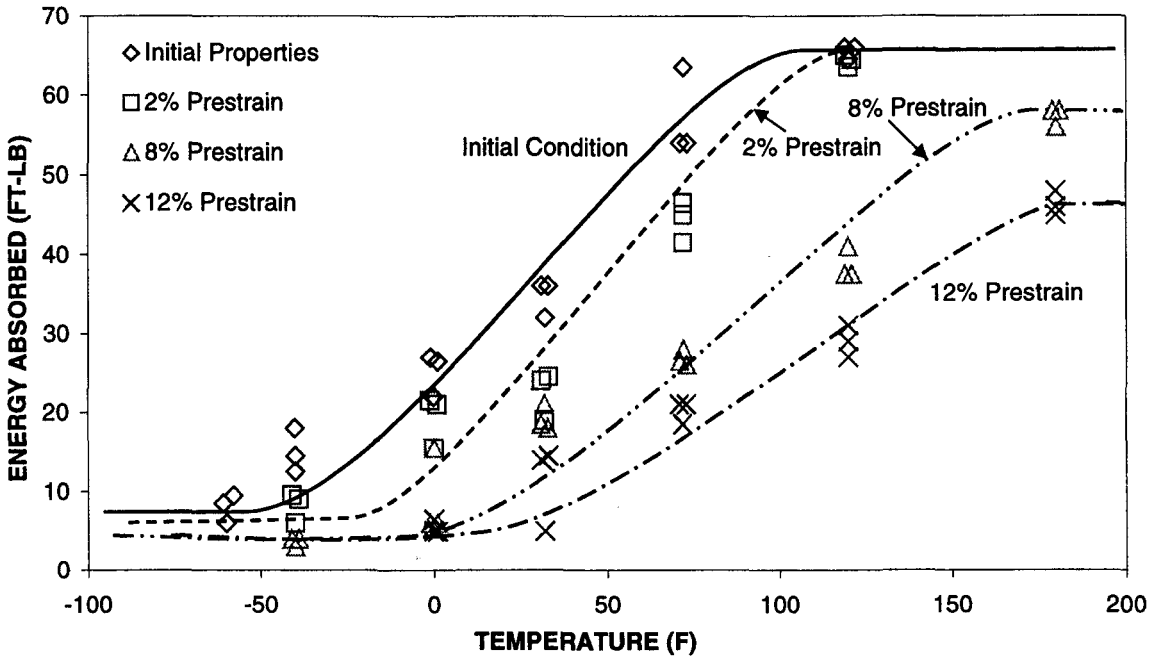

Figure 4E CVN transition curves of Steel C in the TL direction for various prestrain conditions

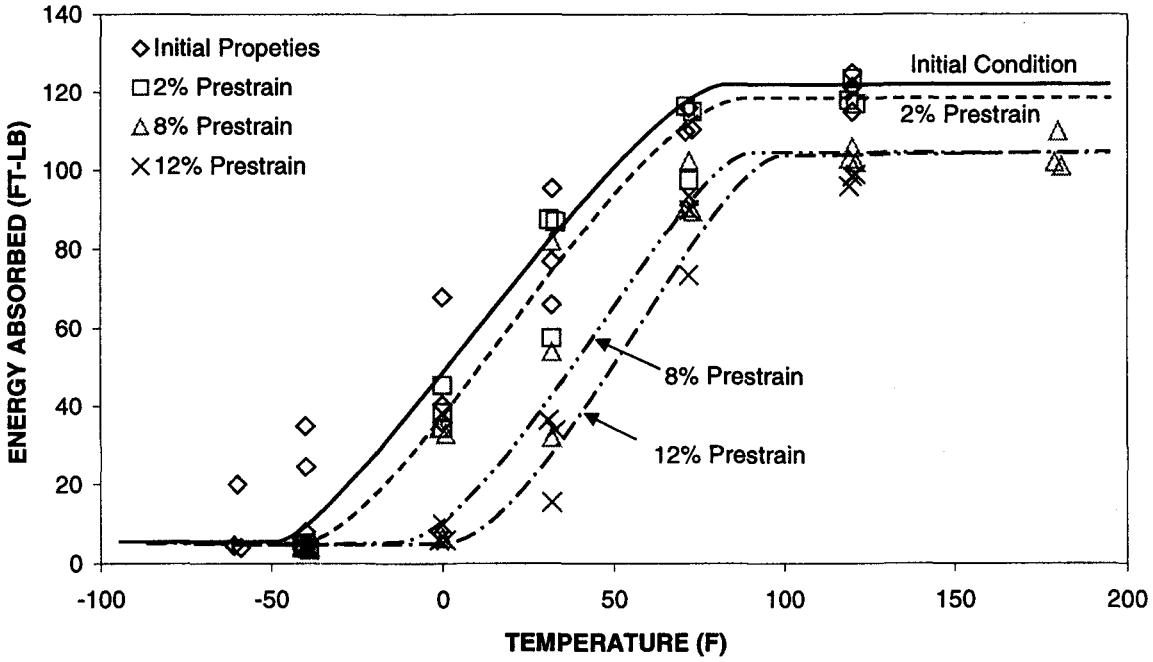

Figure 4F CVN transition curves of Steel C in the LT direction for various prestrain conditions

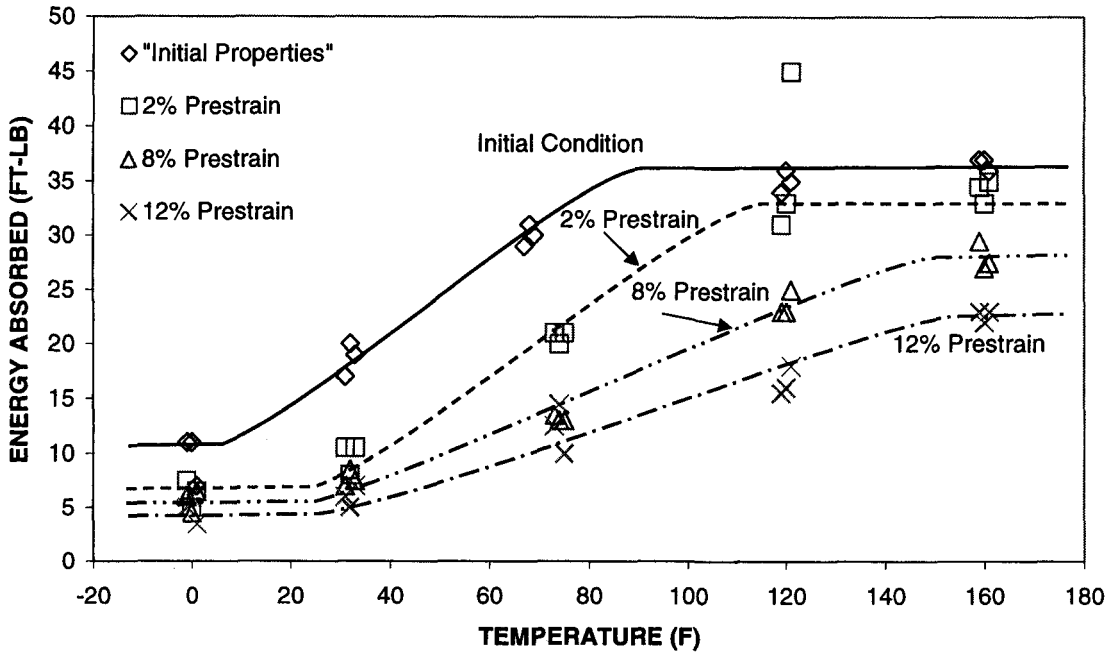

Figure 4G CVN transition curves of Steel D in the TL direction for various prestrain conditions

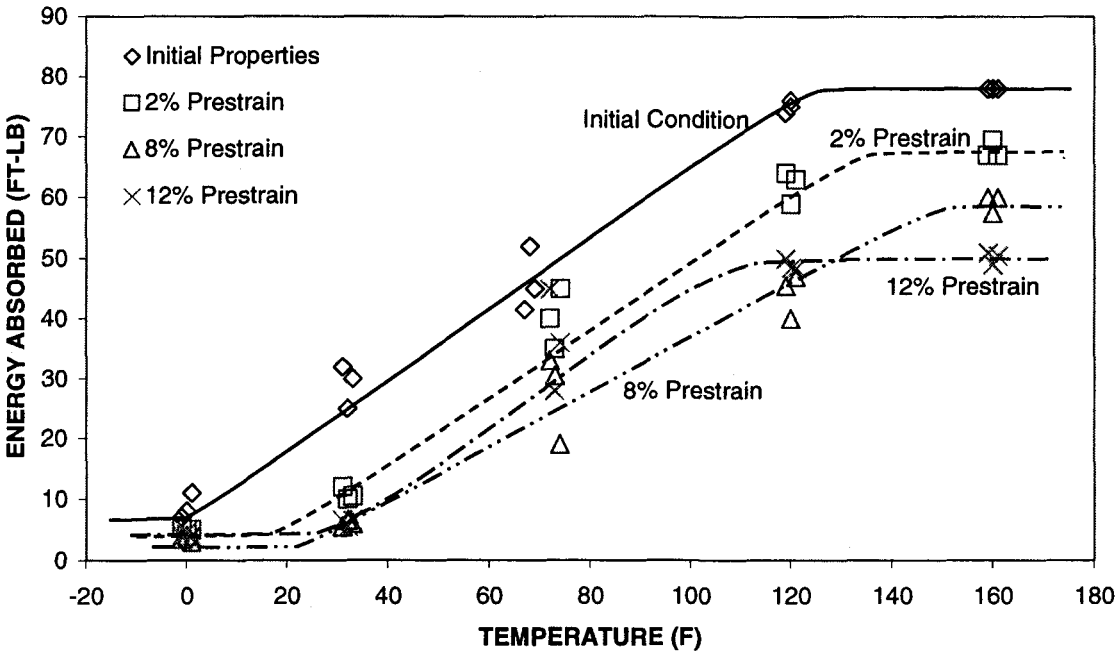

Figure 4H CVN transition curves of Steel D in the LT direction for various prestrain conditions

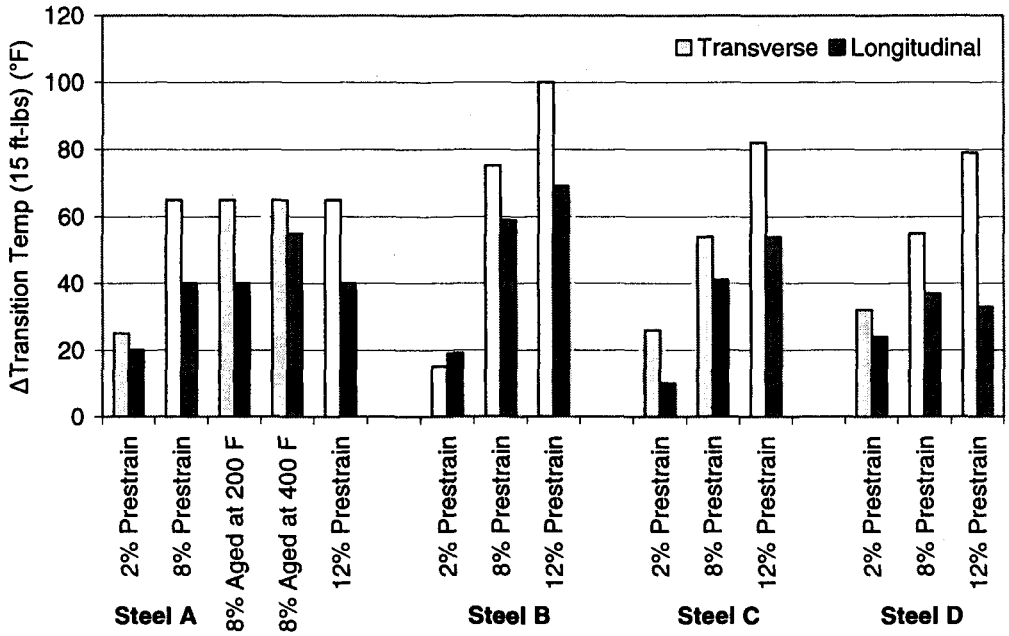

Figure 5 $\Delta T_{transition}$ at 15 ft-lbs from initial condition for various prestrain conditions

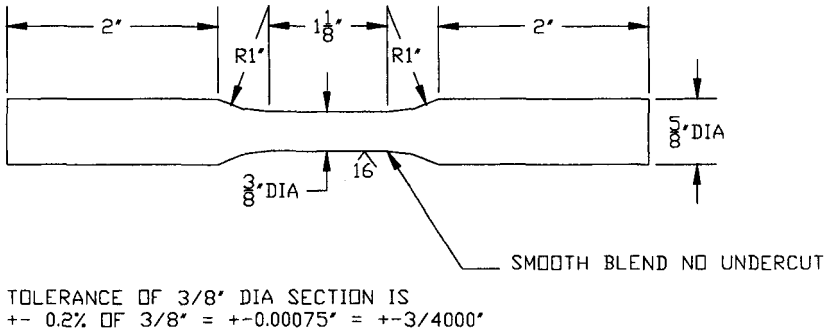

Figure 6 Cyclic strain test specimen (ASTM E606)

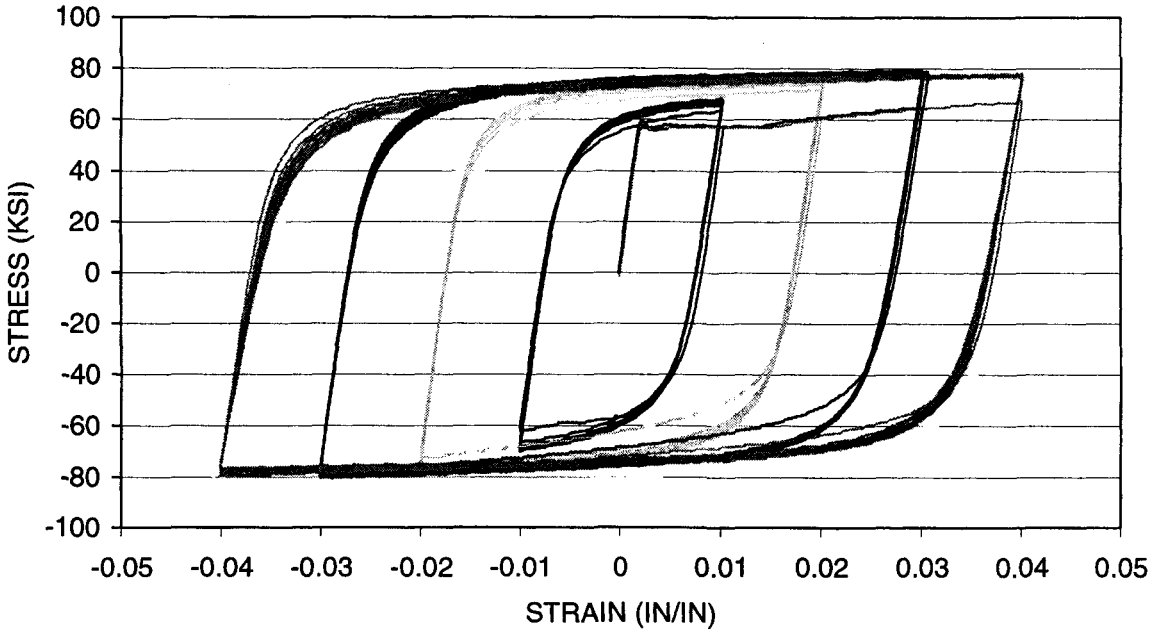

Figure 7A Steel A under cyclic strains of 2%, 4%, 6% and 8% for 10 cycles each

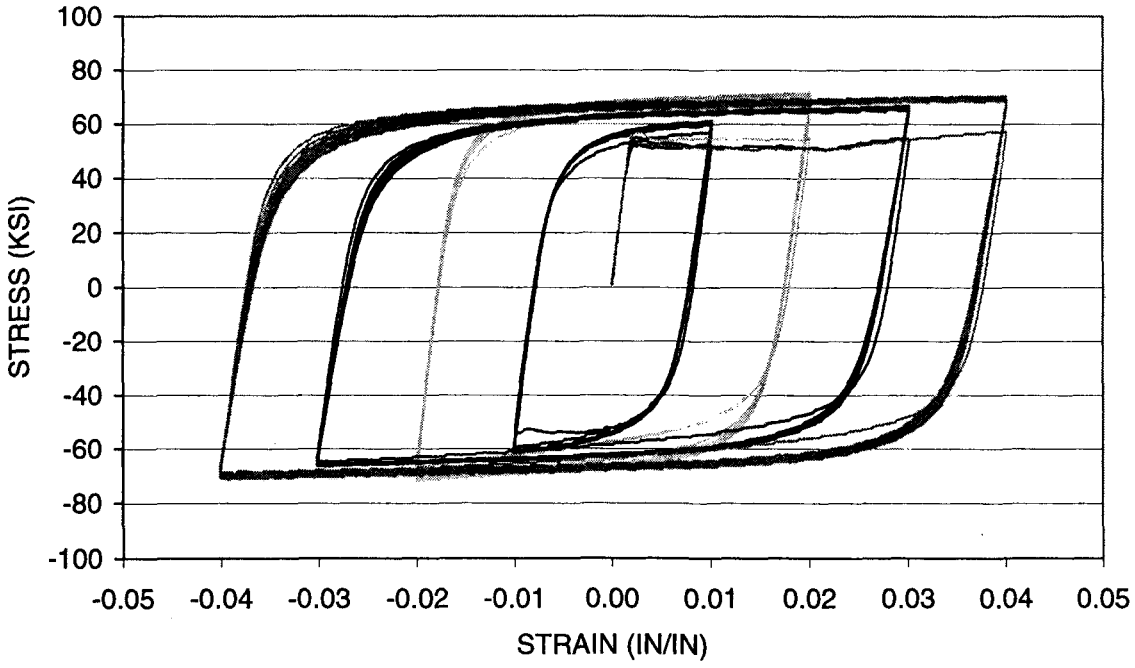

Figure 7B Steel B under cyclic strains of 2%, 4%, 6% and 8% for 10 cycles each

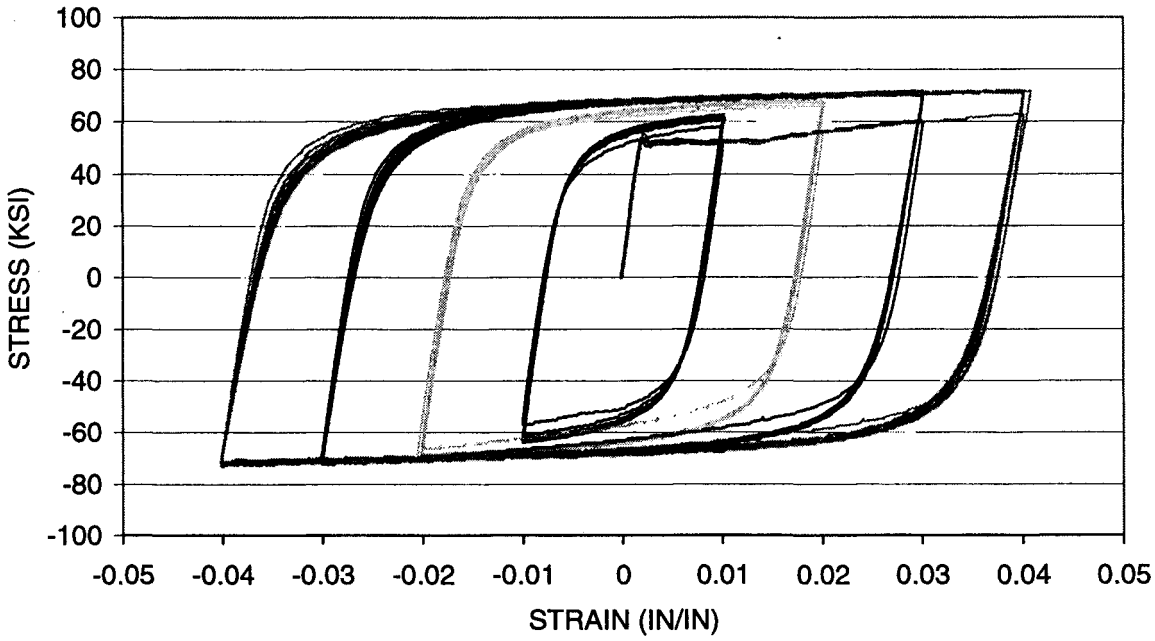

Figure 7C Steel C under cyclic strains of 2%, 4%, 6% and 8% for 10 cycles each

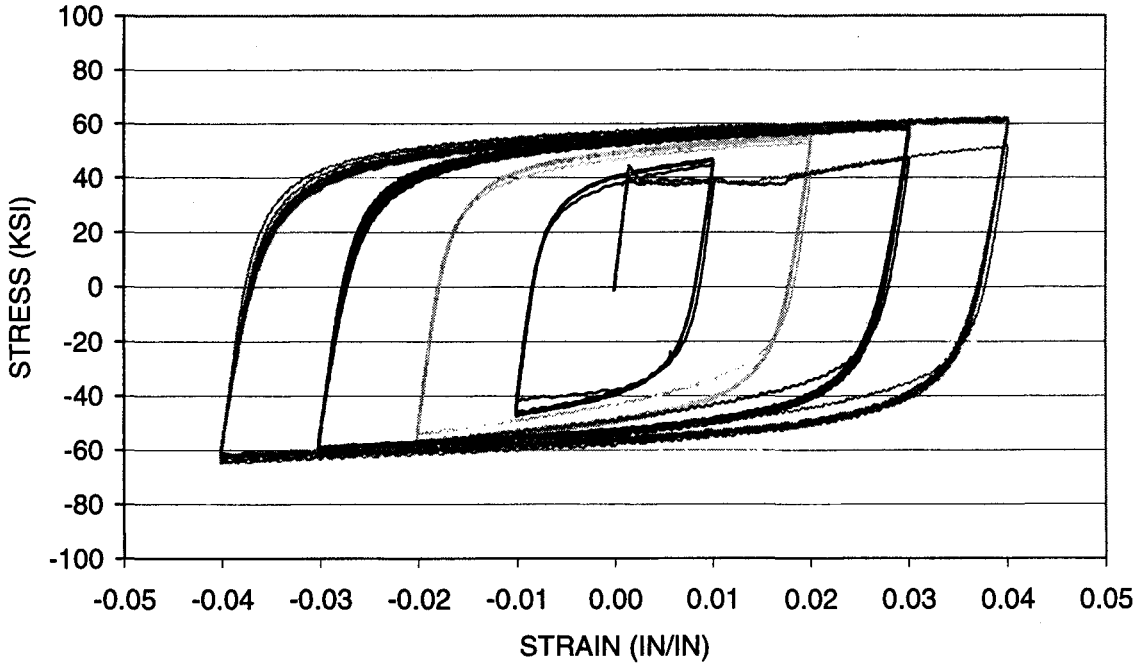

Figure 7D Steel D under cyclic strains of 2%, 4%, 6% and 8% for 10 cycles each

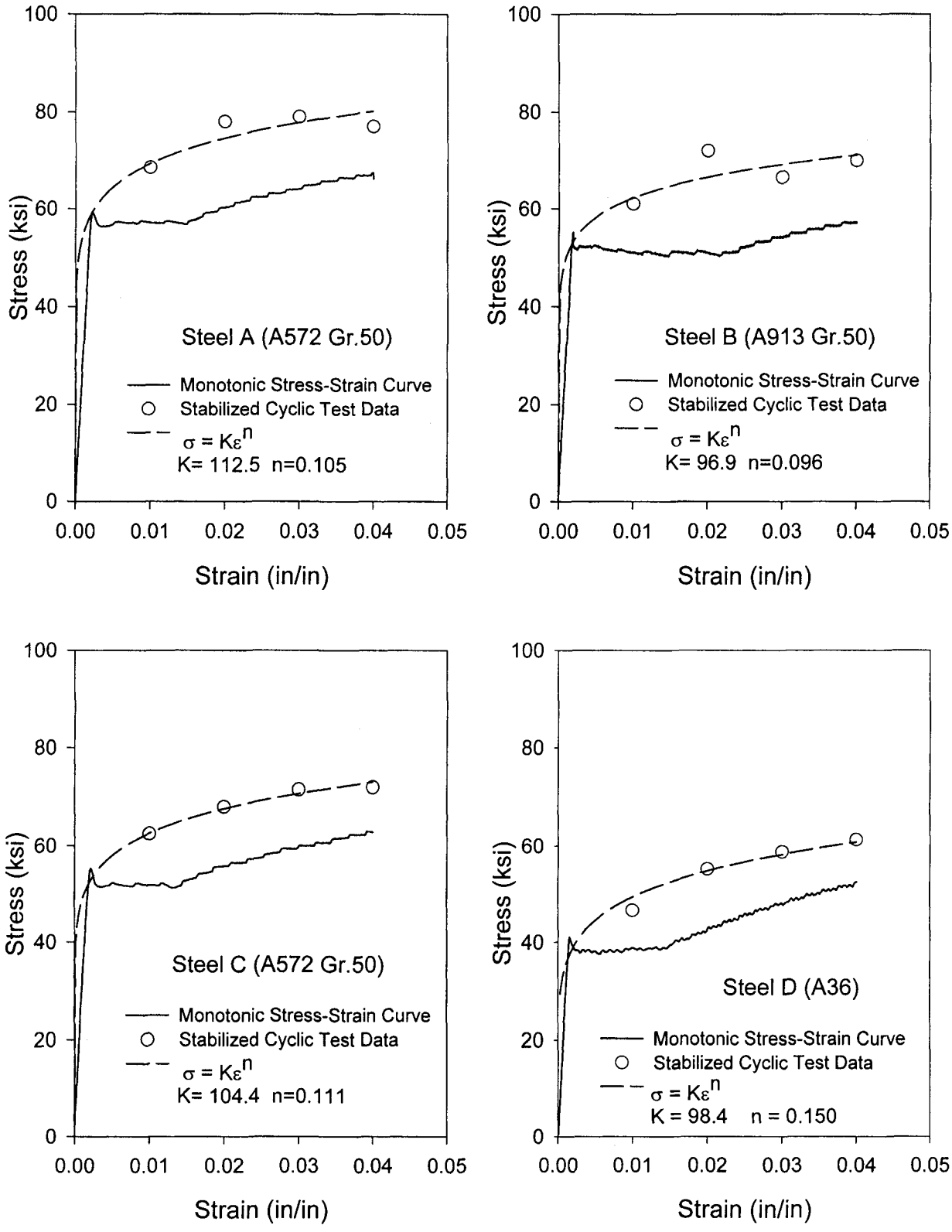

Figure 8 Comparison of monotonic and stabilized cyclic stress-strain behavior of the four steels.

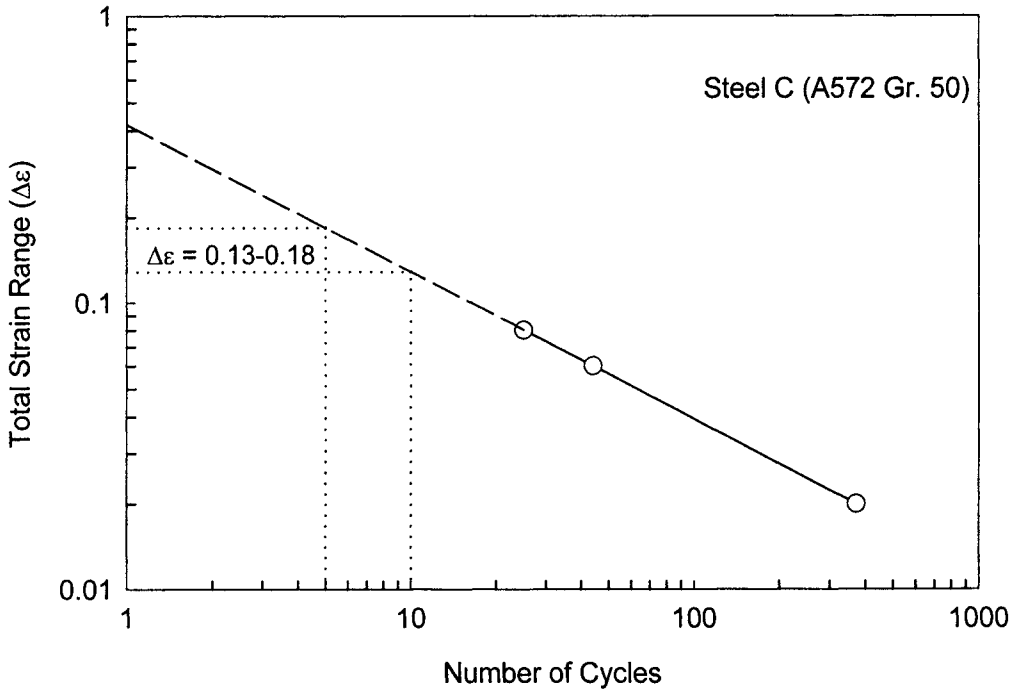

Figure 9 Strain-life plot for for Steel C (A572 Gr. 50) extrapolated to low fatigue life.

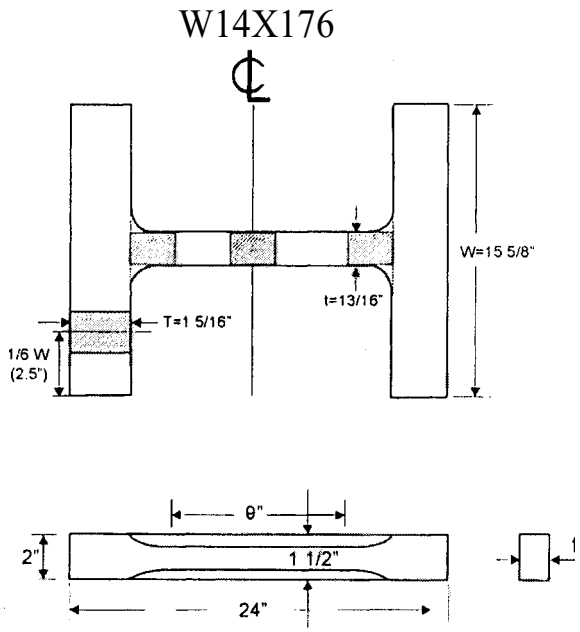

Figure 10 Tensile Coupon Layout.

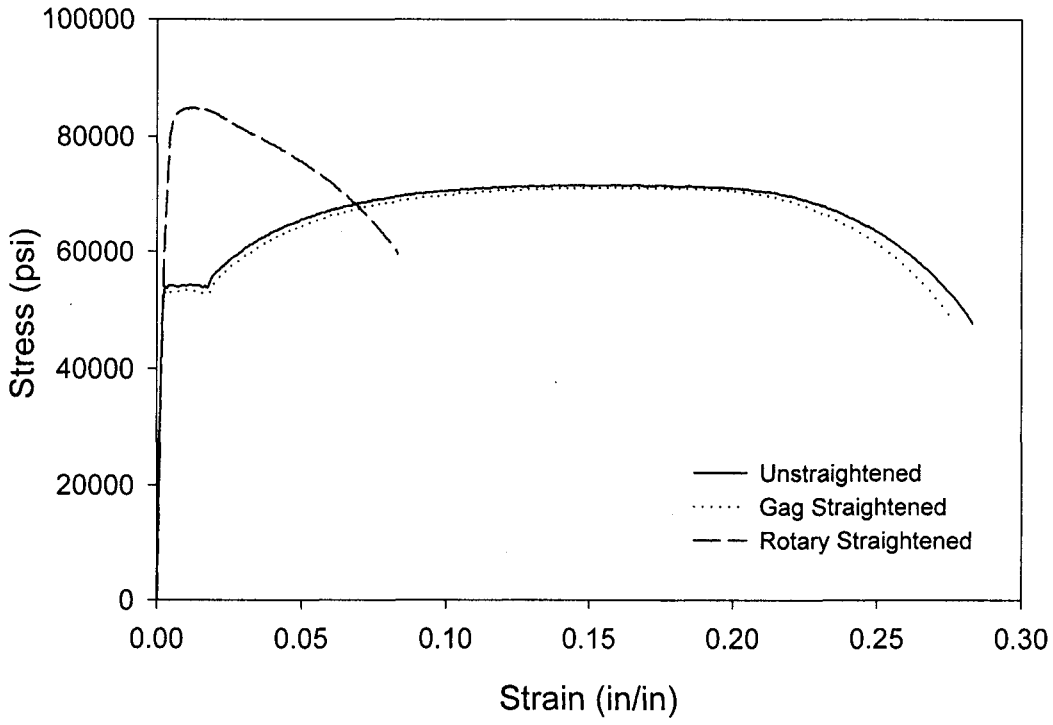

Figure 11 K-area Stress-Strain Behavior for the Three Differently Processed Sections.

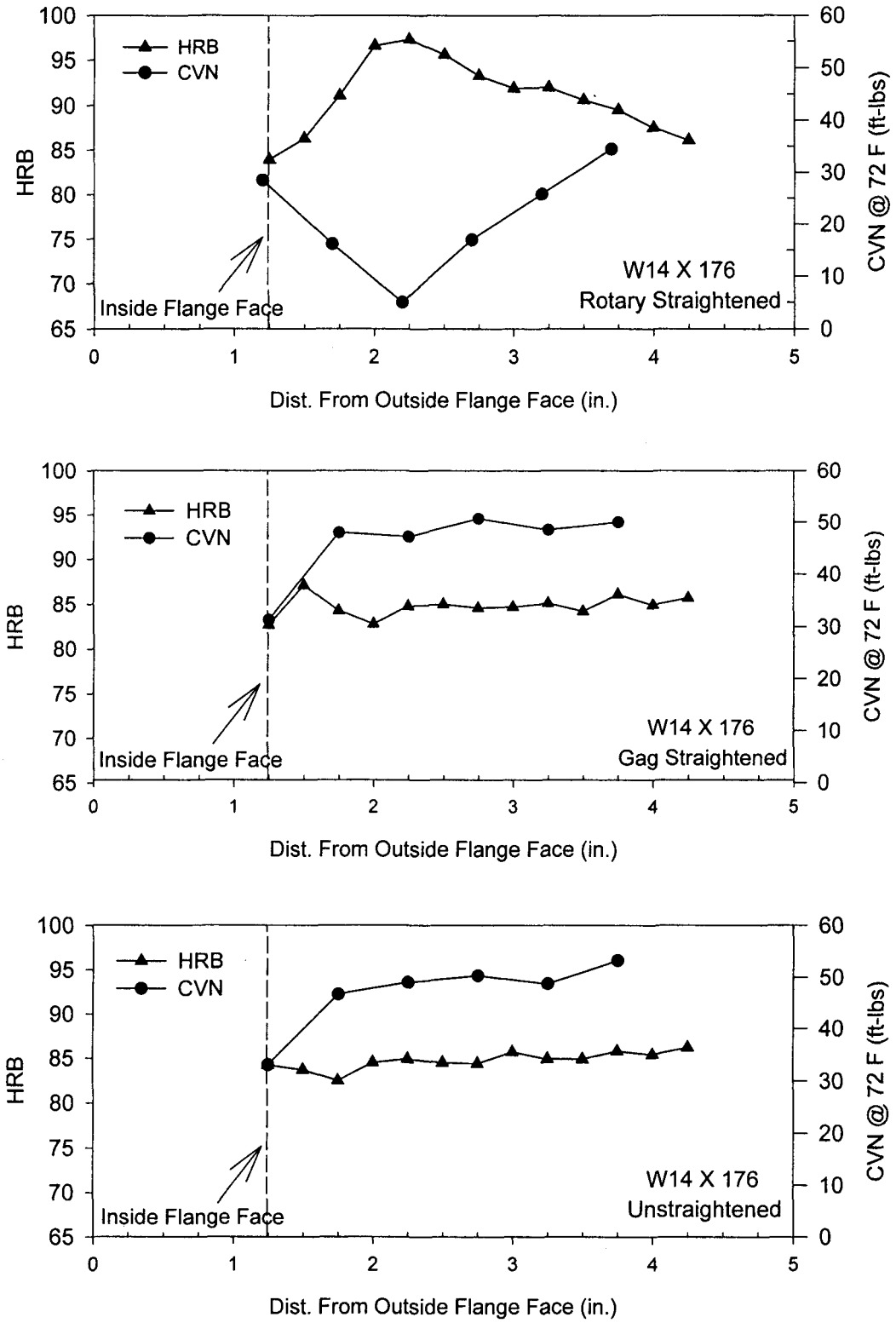

Figure 12 K-area Hardness and CVN for the Three Differently Processed Sections.

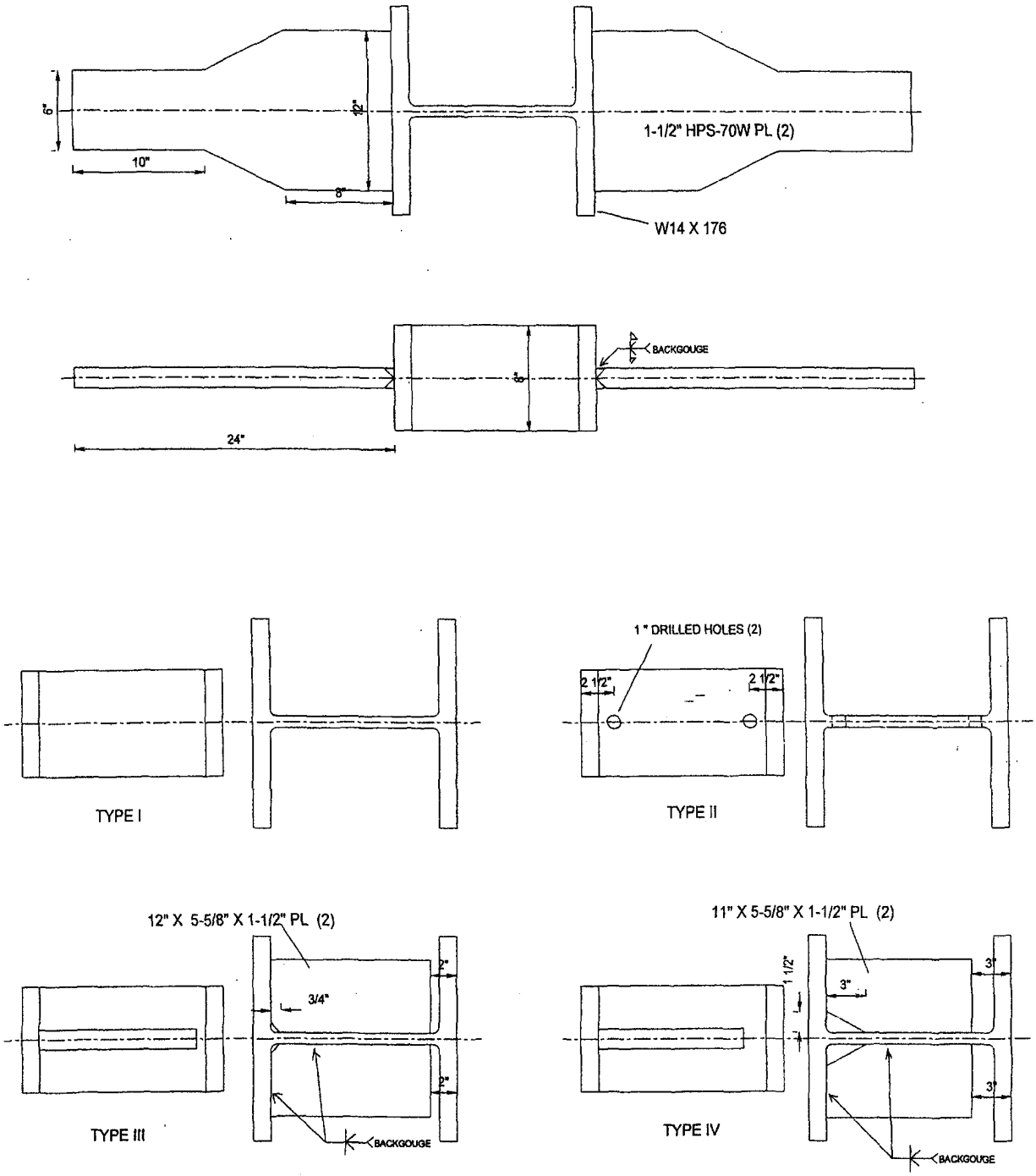

Figure 13 K-area Tension Test Specimen Design and Test Configurations.